Progress In Electromagnetics Research M, Vol. 98, 101–111, 2020

Performance Analysis of Reconfigurable Intelligent Surface Assisted Underwater Optical Communication System

Kehinde O. Odeyemi[1, 2, *], Pius A. Owolawi[1], and Oladayo O. Olakanmi[2]

Abstract—In this paper, the performance analysis of a reconfigurable intelligent surface (RIS) assisted underwater optical communication (UWOC) system with a decode-and-forward (DF) relaying protocol is presented. The radio frequency (RF)-RIS link is subjected to Rayleigh fading while the optical UWOC link experiences mixture Exponential-Gamma distributions subject to heterodyne detection and intensity modulation with direct detection (IMDD). In order to obtain a traceable closed-form expression, the statistical distribution of the RF-RIS link is derived in terms of Meijer-G function. Thus, the exact closed-form expressions for system end-to-end outage probability and average bit error rate (ABER) for different modulation schemes are then derived. To gain further insight about the derived analytical expressions, asymptotic expressions for the system are derived at high signal-to-noise ratio (SNR) through which the diversity gain is obtained. The findings show the significant impact of the number of RIS elements, detection technique, and the UWOC optical turbulence on the system performance. Finally, Monte-Carlo simulation is used to justify the accuracy of the derived analytical results.

1. INTRODUCTION

Recently, reconfigurable intelligent surface (RIS) has been considered as a promising technology for future wireless communication system because it requires no additional power supply, complex encoding and decoding process to achieve high energy and spectrum efficiency [1, 2]. As a result, the quality of the received signal can be simply improved by increasing the number of reflecting elements in RIS [3, 4]. As a new invention, the concept of RIS is based on the use of large number of small, low-cost and passive elements to reflect the incident signal through the adjustable amplitude and phase shift of each reflecting element without signal processing [5, 6]. Based on this, it reduces the blockage effects and significantly improve the system diversity compared to MIMO and amplify-and-forward (AF) relaying counterparts [5, 7]. In literature, RIS is also referred to as intelligent wall [8], smart reflect-array [9], passive intelligent , mirror [1], intelligent reflecting surface [10], and large intelligent surface [11].

In recent years, underwater optical communication (UWOC) system has attracted considerable attention in the research community owing to its capability to provide high transmission speed and reliable communication over short ranges in ocean or seawater channels [12, 13]. As a result, UWOC has found applications in oil exploration, environmental monitoring, port security, oceanographic data collections, etc. Nevertheless, the UWOC channel suffers from absorption, scattering, as well as underwater optical turbulence [14]. Absorption limits the received intensity signal, and the scattering causes misalignment of the transmit beam from the receiver line-of-sight (LOS) [15]. The underwater optical turbulence occurs as a result of variation in the water refractive index due to

Received 12 October 2020, Accepted 3 November 2020, Scheduled 11 November 2020
* Corresponding author: Kehinde O. Odeyemi (kesonics@yahoo.com).
[1] Department of Computer Systems Engineering, Tshwane University of Technology, Pretoria-0001, South Africa. [2] Department of Electrical and Electronic Engineering, Faculty of Technology, University of Ibadan, Nigeria.

change in temperature, salinity variation, and air bubbles which in turn affect the optical signal propagation [14, 16].

Cooperative relaying technique has been suggested in literatures has migration tools to overcome the effect of fading channel in wireless communication system. It involves the use of AF or DF relay node to convey source information to the destination. As a result, it extends the system coverage area and offers better system capacity [17]. Thus, combining the advantages of UWOC and radio frequency (RF) simultaneously is achievable through the relaying technique [18]. Based on this, a few research works have studied the performance of a dual-hop UWOC/RF system over different channel distributions compared to a mixed free space optical (FSO)/RF system [14, 16, 19, 20]. In this case , the performance analysis of a dual-hop RF-UWOC system was evaluated in [20] under the heterodyne and IMDD detection techniques. In [16], a unified statistical model was proposed to characterize the turbulence-induced fading in UWOC channels using experimental data. The average bit error rate and the outage probability performance of a dual-hop underwater system over a mixture exponential-Generalized Gamma turbulence channel was investigated in [14]. Moreover, the performance analysis of UWOC system relayed over the $\alpha - \mu$ fading channel was studied in [19], where outage probability and capacity of the system were obtained. However, all these aforementioned works are based on traditional relaying protocol, and RIS technique was not deployed. By our findings, the research study of a RIS-assisted mixed dual-hop system is still at infancy stage. In [4], a dual-hop RIS-assisted FSO/RF was studied where the RIS was used to enhance the system performance and coverage area, but the work is not UWOC-based system.

Motivated by the above observations, the performance analysis of a reconfigurable intelligent surface assisted underwater optical communication system with a DF relaying protocol under the heterodyne and IMDD detection schemes is presented. To the best of authors' knowledge, no prior work has applied RIS technique to improve the performance of a mixed UWOC/RF system. The RF-RIS link and UWOC link are assumed to follow Rayleigh and mixture Exponential-Gamma distributions, respectively. The system exact closed-form expressions in terms of outage probability and ABER are derived. To gain more physical insight about the system, the asymptotic expressions for the outage probability and ABER are obtained, and the diversity gain of the system is determined. Thus, the main contributions in this study are summarised as follows:

(i) The system analytical closed-form expressions for the outage probability and ABER are derived under the heterodyne and IMDD detection techniques.
(ii) The asymptotic expression for the system outage probability and ABER are determined at high SNR subject to the two detection schemes, and the system diversity gain is obtained.
(iii) Relative to [4] where the RIS was utilized to relay an FSO communication system, this work is based on a UWOC system, and RIS technique was used to improve the system performance.

The remainder of this paper is organized as follows. Section 2 illustrates the concerned system and channel models. The performance analysis of the system with asymptotic analysis is presented in Section 3. In Section 4, the numerical results with insightful discussions are presented. Finally, Section 5 gives conclusion remarks of the paper.

2. SYSTEM AND CHANNEL MODELS

The RIS-relayed underwater optical system model is illustrated in Figure 1, where the source (S) (i.e., drone or diver) sends its information to the destination (D) via the relay (R) (i.e., ship) and the RIS. S, R, and D are equipped with a single antenna or aperture while the RIS consists of N number of reflecting elements with full knowledge of channel state information of the channel. It is assumed that there is no direct link between the relay and destination due to blockage which causes the RIS to form an intelligent environment for the signal quality enhancement. This is achieved by optimizing the phases of the reflecting signal without additional power. Since the system is cooperative-based, the transmission of information occurs in two phases, and the system operates in half duplex mode. During the first phase, the source transmits its information via the optical link to the relay, and the optical signal received by the relay can be expressed as:

$$y_R^{opt} = \eta h_{SR} \left\{ \sqrt{P_S^{opt}} \left(1 + M x_S\right) \right\} + z_R^{opt}(t) \tag{1}$$

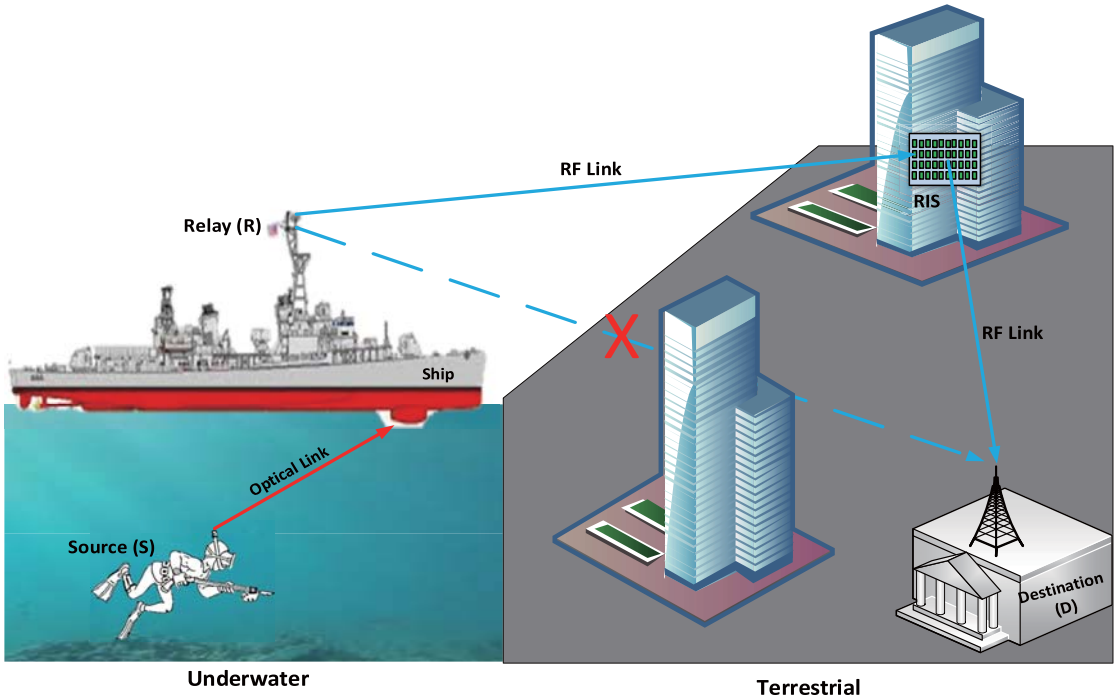

Figure 1. RIS-relayed UWOC system model.

where h_{SR} is the channel gain between S and R; η represents the optical-electrical conversion coefficient; P_S^{opt} denotes the optical transmit power; M signifies the modulation index; x_S is the source information; z_R^{opt} is the additive white Gaussian noise (AWGN) at the relay with σ_R^2 variance. Thus, the instantaneous SNR at the relay can be expressed as:

$$\gamma_R = \bar{\gamma}_{SR} \left|h_{SR}\right|^2 \tag{2}$$

where $\bar{\gamma}_{SR} = \eta P_S^{opt}/\sigma_R^2$ denotes the average SNR at the relay.

During the second phase, the relay transmits the received source signal to the destination after converting the optical signal to the electrical signal. The received signal at the destination can then be expressed as:

$$y_D^{RF} = \sqrt{P}_R^{RF} \left\{ \sum_{i=1}^{N} h_i \exp\left(j\phi_i\right) g_i \right\} x_R + z_D^{RF}\left(t\right) \tag{3}$$

where ϕ_i denotes the adjustable phase induced by i-th reflector elements; P_R^{RF} is the relay transmit power; x_R is the source information transmitted by the relay; $z_D^{RF}(t)$ is the AWGN at the destination with σ_D^2 variance. Also, $h_i = \nu_i \exp(-j\theta_i)$ and $g_i = u_i \exp(-j\psi_i)$ are the channel gains of the R-RIS and RIS-D links, respectively with ν_i and u_i being the amplitudes of the Rayleigh distribution, respective, and θ_i and ψ_i are the phases. In order to eliminate the channel phase, $\phi_i = \theta_i + \psi_i$ so as to maximised the SNR at the destination. Thus, the instantaneous SNR at the destination can then be expressed as:

$$\gamma_D = \bar{\gamma}_{RD} \left(\sum_{i=1}^{N} \nu_i u_i \right)^2 \tag{4}$$

where $\bar{\gamma}_{RD} = P_R^{RF}/\sigma_D^2$ represents the average SNR at the destination.

2.1. UWOC Statistic Channel

The optical turbulence of UWOC link is assumed to follow the mixture Exponential-Gamma distributions which is known as thermally uniform UWOC channel, and the cumulative density function

(CDF) can be expressed as [16, 20]:

$$F_{\gamma_{SR}}\left(\gamma_{SR}\right)=\sum_{j=1}^{2}A_jG_{1,2}^{1,1}\left(B_j\gamma_{SR}^{1/r}\Big|_{C_j,\,0}^{1}\right) \tag{5}$$

where $A_1=\omega$ and $A_2=\left(1-\omega\right)/\Gamma\left(\alpha\right)$, $B_1=1/\lambda\mu_r^{1/r}$ and $B_1=1/\beta\mu_r^{1/r}$, $C_1=1$ and $C_2=\alpha$, $\mu_1=\bar{\gamma}_{SR}$ and $\mu_2=\frac{\bar{\gamma}_{SR}}{2\omega\lambda^2+\beta^2(1-\omega)\Gamma(\alpha+2)/\Gamma(\alpha)}$ are the average electrical SNR for the heterodyne detection and IM/DD, respectively. ω is the mixture weight of the distributions, $0<\omega<1$; λ is the exponential distribution parameter; α and β are shape and scale parameters of the Gamma distribution. The values of $\omega\lambda$, α, and β under different air bubbles levels (BL) and temperature gradients (T) are defined in [16]. The probability density function (PDF) of the UWOC can then be obtained by differential Eq. (5) using the identity detail in [24] as:

$$f_{\gamma_{SR}}\left(\gamma_{SR}\right)=\sum_{j=1}^{2}D_j\gamma_{SR}^{-1}G_{0,1}^{1,0}\left(B_j\gamma_{SR}^{1/r}\Big|_{C_j}^{-}\right) \tag{6}$$

where $D_1=\omega/r$ and $D_2=\left(1-\omega\right)/\mathrm{r}\Gamma\left(\alpha\right)$.

2.2. RF-RIS Statistic Channel

In this paper, the RF-RIS link is assumed to follow Rayleigh distribution, and thus ν_i and u_i are independently Rayleigh distributed random variables. From Eq. (4), let $H=\sum\limits_{i=1}^{N}\nu_iu_i$, then according to the central limit theorem for large N [21], H follows Gaussian distribution with $H\sim N\left(\frac{N\pi}{4},\frac{N\left(16-\pi^2\right)}{16}\right)$. Therefore, the instantaneous SNR of the RF-RIS link is a non-central chi-square random variable with one degree of freedom, and its PDF is given by [2, 22]:

$$f_{\gamma_{RD}}\left(\gamma_{RD}\right)=\frac{1}{2\xi^2}\left(\frac{\gamma_{RD}}{\rho}\right)^{-1/4}\exp\left(-\frac{\gamma_{RD}+\rho}{2\xi^2}\right)I_{-1/2}\left(\frac{\sqrt{\gamma_{RD}\rho}}{\xi^2}\right) \tag{7}$$

where $\xi^2=\bar{\gamma}N\left(16+\pi^2\right)/16$, $\rho=\bar{\gamma}\pi^2N^2/16$, and $I_n\left(.\right)$ denotes the modified Bessel function of first order.

By utilizing the identity defined in [23], the modified Bessel function of first order can thus be expressed in terms of Meijer-G function as follows:

$$I_{-1/2}\left(\frac{\sqrt{\gamma_{RD}\rho}}{\xi^2}\right)=\pi\sqrt{2}\rho^{-1/4}\gamma_{RD}^{-1/4}G_{1,3}^{1,0}\left(\frac{\rho}{4\xi^4}\gamma_{RD}\Big|_{0,\,1/2,\,1/2}^{1/2}\right) \tag{8}$$

Putting Eq. (8) into Eq. (7), the link PDF can be further expressed as:

$$f_{\gamma_{RD}}\left(\gamma_{RD}\right)=\frac{\pi\sqrt{2}}{2\xi}\exp\left(-\frac{\rho}{2\xi^2}\right)\exp\left(-\frac{\gamma_{RD}}{2\xi^2}\right)\gamma_{RD}^{-1/8}G_{1,3}^{1,0}\left(\frac{\rho}{4\xi^4}\gamma_{RD}\Big|_{0,\,1/2,\,1/2}^{1/2}\right) \tag{9}$$

By using infinite series of exponential function detailed in [24, Eq. (1.211(3))] as $\exp\left(-\frac{\gamma_{RD}}{2\xi^2}\right)=\sum\limits_{k=0}^{\infty}\frac{(-1)^k}{k!(2\xi^2)^k}\gamma_{RD}^k$, the link PDF can be written as:

$$f_{\gamma_{RD}}\left(\gamma_{RD}\right)=\frac{\pi\sqrt{2}}{2\xi}\exp\left(-\frac{\rho}{2\xi^2}\right)\sum_{k=0}^{\infty}\frac{\left(-1\right)^k}{k!\left(2\xi^2\right)^k}\gamma_{RD}^{k-1/8}G_{1,3}^{1,0}\left(\frac{\rho}{4\xi^4}\gamma_{RD}\Big|_{0,\,1/2,\,1/2}^{1/2}\right) \tag{10}$$

By making use of integral identity defined in [25, Eq. (26)], the link CDF can be obtained as:

$$F_{\gamma_{RD}}\left(\gamma_{RD}\right)=\frac{\pi\sqrt{2}}{2\xi}\exp\left(-\frac{\rho}{2\xi^2}\right)\sum_{k=0}^{\infty}\frac{\left(-1\right)^k}{k!\left(2\xi^2\right)^k}\gamma_{RD}^{k+7/8}G_{2,4}^{1,1}\left(\frac{\rho}{4\xi^4}\gamma_{RD}\Big|_{0,\,\left(-k-7/8\right),\,1/2,\,1/2}^{1/2,\,\left(1/8-k\right)}\right) \tag{11}$$

3. PERFORMANCE ANALYSIS

3.1. Outage Probability Analysis

Outage Probability is an important indicator in wireless systems which describes the probability that instantaneous SNR falls below a predefined threshold value γ_{th}. Thus, the end-to-end outage probability for the concerned system can be expressed as [19, 26]:

$$\begin{aligned} P_{out}\left(\gamma_{th}\right) &= P_r\left(\gamma_{SR} < \gamma_{th} or \gamma_{RD} < \gamma_{th}\right) \\ &\triangleq 1 - \left(1 - P_r\left(\gamma_{SR} < \gamma_{th}\right)\right)\left(1 - P_r\left(\gamma_{RD} < \gamma_{th}\right)\right) \\ &\triangleq F_{\gamma_{SR}}^{Opt}\left(\gamma_{th}\right) + F_{\gamma_{RD}}^{RF}\left(\gamma_{th}\right) - F_{\gamma_{SR}}^{Opt}\left(\gamma_{th}\right) F_{\gamma_{RD}}^{RF}\left(\gamma_{th}\right) \end{aligned} \tag{12}$$

By invoking Eqs. (5) and (11) into Eq. (12), the system outage probability can be thus be obtained:

$$\begin{aligned} P_{out}\left(\gamma_{th}\right) = & \sum_{j=1}^{2} A_j G_{1,2}^{1,1}\left(B_j \gamma_{th}^{1/r}\middle|\begin{matrix}1\\ C_j, 0\end{matrix}\right) \\ & + \frac{\pi\sqrt{2}}{2\xi}\exp\left(-\frac{\rho}{2\xi^2}\right)\sum_{k=0}^{\infty}\frac{(-1)^k}{k!\left(2\xi^2\right)^k}\gamma_{th}^{k+7/8} G_{2,4}^{1,1}\left(\frac{\rho}{4\xi^4}\gamma_{th}\middle|\begin{matrix}1/2, (1/8-k)\\ 0, (-k-7/8), 1/2, 1/2\end{matrix}\right) \\ & - \frac{\pi\sqrt{2}}{2\xi}\exp\left(-\frac{\rho}{2\xi^2}\right)\sum_{k=0}^{\infty}\sum_{j=1}^{2}\frac{A_j(-1)^k}{k!\left(2\xi^2\right)^k}\gamma_{th}^{k+7/8} G_{1,2}^{1,1}\left(B_j\gamma_{th}^{1/r}\middle|\begin{matrix}1\\ C_j, 0\end{matrix}\right) \\ & G_{2,4}^{1,1}\left(\frac{\rho}{4\xi^4}\gamma_{th}\middle|\begin{matrix}1/2, (1/8-k)\\ 0, (-k-7/8), 1/2, 1/2\end{matrix}\right) \end{aligned} \tag{13}$$

3.2. Asymptotic Outage Probability Analysis

The exact outage probability closed-form expression derived in Eq. (13) cannot show explicit insight about the concerned system as a result of its complexity. Therefore, asymptotic analysis provides more insights of the effect of different system parameters on the system outage performance. At high SNR, the system end-to-end outage expression can be defined as [27]:

$$P_{out}^{Asy}\left(\gamma\right) \approx F_{\gamma_{SR}}^{Opt,Asy}\left(\gamma\right) + F_{\gamma_{RD}}^{RF,Asy}\left(\gamma\right) \tag{14}$$

where $F_{\gamma_{SR}}^{Opt,Asy}\left(\gamma\right)$ and $F_{\gamma_{RD}}^{RF,Asy}\left(\gamma\right)$ are the CDF of UWOC and RF link at high SNR, respectively.

To determine the CDF for each system link at high SNR, the asymptotic series expansion of the Meijer-G function at zero can be expressed as [6, 24]:

$$G_{p,q}^{m,n}\left(z\middle|\begin{matrix}a_1, \ldots a_n, a_{n+1} \ldots a_p\\ b_1, \ldots b_m, b_{m+1} \ldots b_q\end{matrix}\right) = \sum_{l=1}^{m}\frac{\prod\limits_{\substack{g=1\\ l\neq t}}^{m}\Gamma\left(b_t - b_l\right)\prod\limits_{t=1}^{n}\Gamma\left(1 - a_l + b_t\right)}{\prod\limits_{t=n+1}^{p}\Gamma\left(a_t - b_l\right)\prod\limits_{t=m+1}^{q}\Gamma\left(1 - b_t + b_l\right)} z^{b_l} \tag{15}$$

where $p \geq q$, and $z \to 0$ is assumed.

Thus, the CDF for the UWOC link at high SNR can be obtained by applying Eqs. (15) to (5) as follows:

$$F_{\gamma_{SR}}^{Opt,Asy}\left(\gamma\right) = \sum_{j=1}^{2} A_j\left(B_j\gamma^{1/r}\right)^{C_j}\frac{\Gamma\left(C_j\right)}{\Gamma\left(1 + C_j\right)} \tag{16}$$

Following the same approach as in the case of Eq. (16), the CDF of RIS link can be obtained as:

$$F_{\gamma_{RD}}^{RF,Asy}\left(\gamma\right) = \frac{\pi\sqrt{2}}{2\xi}\exp\left(-\frac{\rho}{2\xi^2}\right)\sum_{k=0}^{\infty}\frac{(-1)^k}{k!\left(2\xi^2\right)^k\Gamma\left(k + 15/8\right)\Gamma\left(1/8 - k\right)\Gamma\left(1/2\right)}\gamma^{k+7/8} \tag{17}$$

Therefore, by putting Eqs. (16) and (17) into Eq. (14), the system asymptotic outage probability at high SNR can be obtained as:

$$P_{out}^{Asy}(\gamma) = \sum_{j=1}^{2} A_j \left(B_j \gamma^{1/r}\right)^{C_j} \frac{\Gamma(C_j)}{\Gamma(1+C_j)} + \frac{\pi\sqrt{2}}{2\xi} \exp\left(-\frac{\rho}{2\xi^2}\right) \times \sum_{k=0}^{\infty} \frac{(-1)^k}{k!\,(2\xi^2)^k\,\Gamma(k+15/8)\,\Gamma(1/8-k)\,\Gamma(1/2)} \gamma^{k+7/8} \tag{18}$$

Hence, the system diversity order can be obtained as:

$$G_d = -\lim_{\gamma\to\infty} \frac{\ln P_{out}^{Asy}(\gamma)}{\ln \bar{\gamma}} \triangleq \min\left(k, \frac{C_j}{r}\right) \tag{19}$$

3.3. Average Bit Error Rate Analysis

In this work, the system is a DF-based relaying system, and the ABER can be obtained through the unified error rate expression for different forms of modulation schemes defined as in [18, 19]:

$$ABER = P_{E_1}^{Opt} + P_{E_2}^{RF} - 2P_{E_1}^{Opt} P_{E_2}^{RF} \tag{20}$$

where

$$P_{E_\tau}^{i} = \frac{p\sqrt{q}}{2\sqrt{\pi}} \int_0^\infty \gamma^{-1/2} \exp(-q\gamma)\, F_{\gamma_{SR}}^{Opt}(\gamma)\, d\gamma, \quad \tau = 1, 2 \tag{21}$$

where $i \in \{Opt, RF\}$, and p and q are the modulation parameters which denote binary phase shift keying (BPSK) when $p = 1$ and $q = 1$ and signify binary frequency shift keying (BFSK) when $p = 1$ and $q = 1/2$.

The ABER for the UWOC link can be determine by putting Eq. (5) into Eq. (21) as:

$$P_{E_1}^{Opt} = \frac{p\sqrt{q}}{2\sqrt{\pi}} \sum_{j=1}^{2} A_j \int_0^\infty \gamma^{-1/2} \exp(-q\gamma)\, G_{1,2}^{1,1}\left(B_j \gamma_{RD}^{1/r} \Big|_{C_j, 0}^{1}\right) d\gamma \tag{22}$$

By converting the exponential function to Meijer-G function using the identity detailed in [25, Eq. (11)], then Eq. (22) can be further expressed as:

$$P_{E_1}^{Opt} = \frac{p\sqrt{q}}{2\sqrt{\pi}} \sum_{j=1}^{2} A_j \int_0^\infty \gamma^{-1/2} G_{0,1}^{1,0}\left(q\gamma \Big|_{0}^{-}\right) G_{1,2}^{1,1}\left(B_j \gamma_{RD}^{1/r} \Big|_{C_j, 0}^{1}\right) d\gamma \tag{23}$$

By applying the integral identity given in [25, Eq. (26)], Eq. (23) can be solved as:

$$P_{E_1}^{Opt} = \frac{p r^{C_j - 1/2}}{2\sqrt{\pi}\left(\sqrt{2\pi}\right)^{r-1}} \sum_{j=1}^{2} A_j G_{r+1,2r}^{r,r+1}\left(\frac{(B_j)^r}{q r^r} \Big|_{\Delta(r, C_j), \Delta(r, 0)}^{\Delta(r,1), 1/2}\right) \tag{24}$$

where $\Delta(x, y) = \frac{x}{y}, \frac{x+1}{y}, \ldots, \frac{x+y-1}{y}$.

The ABER for the RF link can be determined by putting Eq. (11) into Eq. (21) as:

$$P_{E_2}^{RF} = \frac{\pi\sqrt{2q}p}{4\xi\sqrt{\pi}} \exp\left(-\frac{\rho}{2\xi^2}\right) \sum_{k=0}^{\infty} \frac{(-1)^k}{k!\,(2\xi^2)^k} \int_0^\infty \gamma^{k+7/8} \exp(-q\gamma)\, G_{2,4}^{1,1}\left(\frac{\rho}{4\xi^4}\gamma \Big|_{0, (-k-7/8), 1/2, 1/2}^{1/2, (1/8-k)}\right) d\gamma \tag{25}$$

By applying the integral identity detailed in [24, Eq. (7.813(1))], the RF link ABER can be obtained as

$$P_{E_2}^{RF} = \frac{\pi\sqrt{2}p}{4\xi\sqrt{\pi}} \exp\left(-\frac{\rho}{2\xi^2}\right) \sum_{k=0}^{\infty} \frac{(-1)^k q^{-(k+7/8)}}{k!\,(2\xi^2)^k} G_{3,4}^{1,2}\left(\frac{\rho}{4\xi^4}\gamma \Big|_{0, (-k-7/8), 1/2, 1/2}^{(-k-3/8), 1/2, (1/8-k)}\right) \tag{26}$$

Thus, the system end-to-end ABER can be obtained by putting Eqs. (24) and (26) into Eq. (20) as follows:

$$\begin{aligned} ABER \;=\; & \frac{pr^{C_j-1/2}}{2\sqrt{\pi}\left(\sqrt{2\pi}\right)^{r-1}}\sum_{j=1}^{2}A_j G_{r+1,2r}^{r,r+1}\left(\frac{(B_j)^r}{qr^r}\middle|\begin{matrix}\Delta(r,1),1/2\\ \Delta(r,C_j),\Delta(r,0)\end{matrix}\right) \\ & +\frac{\pi\sqrt{2}p}{4\xi\sqrt{\pi}}\exp\left(-\frac{\rho}{2\xi^2}\right)\sum_{k=0}^{\infty}\frac{(-1)^k q^{-(k+7/8)}}{k!\,(2\xi^2)^k}G_{3,4}^{1,2}\left(\frac{\rho}{4\xi^4}\gamma\middle|\begin{matrix}(-k-3/8),1/2,(1/8-k)\\ 0,(-k-7/8),1/2,1/2\end{matrix}\right) \\ & -\frac{\sqrt{2}p^2 r^{C_j-1/2}}{4\xi\left(\sqrt{2\pi}\right)^{r-1}}\exp\left(-\frac{\rho}{2\xi^2}\right)\sum_{j=1}^{2}\sum_{k=0}^{\infty}\frac{(-1)^k q^{-(k+7/8)}A_j}{k!\,(2\xi^2)^k} \\ & \times G_{r+1,2r}^{r,r+1}\left(\frac{(B_j)^r}{qr^r}\middle|\begin{matrix}\Delta(r,1),1/2\\ \Delta(r,C_j),\Delta(r,0)\end{matrix}\right)G_{3,4}^{1,2}\left(\frac{\rho}{4\xi^4}\gamma\middle|\begin{matrix}(-k-3/8),1/2,(1/8-k)\\ 0,(-k-7/8),1/2,1/2\end{matrix}\right) \end{aligned} \tag{27}$$

3.4. Asymptotic Average Bit Error Rate Analysis

Following the same approach as in the case of outage probability, the asymptotic expression of the RF-RIS link error rate can be obtained by using Eq. (16) in Eq. (21) as follows:

$$P_{E_1}^{Opt,Asy}=\frac{p\sqrt{q}}{2\sqrt{\pi}}\sum_{j=1}^{2}A_j\,(B_j)^{C_j}\int_0^{\infty}\frac{\Gamma(C_j)}{\Gamma(1+C_j)}\gamma^{C_j/r-1/2}\exp(-q\gamma)\,d\gamma \tag{28}$$

By applying the integral identity given in [24, Eq. (3.326(2))], Eq. (28) can be solved as:

$$P_{E_1}^{Opt,ASy}=\frac{p}{2\sqrt{\pi}}\sum_{j=1}^{2}A_j\,(B_j)^{C_j}\frac{\Gamma(C_j)\,\Gamma(C_j/2+1/2)}{q^{(C_j/2)}\Gamma(1+C_j)} \tag{29}$$

Similarly, by using Eq. (17) in Eq. (21), the asymptotic expression of the UWOC link error rate can be expressed as:

$$P_{E_2}^{RF,ASy}=\frac{\pi\sqrt{2q}p}{4\xi\sqrt{\pi}}\exp\left(-\frac{\rho}{2\xi^2}\right)\sum_{k=0}^{\infty}\frac{(-1)^k}{k!\,(2\xi^2)^k\,\Gamma(k+15/8)\,\Gamma(1/8-k)\,\Gamma(1/2)}\int_0^{\infty}\gamma^{k+7/8}\exp(-q\gamma)d\gamma \tag{30}$$

Then, by utilizing the integral identity detailed in [24, Eq. (3.326(2))], Eq. (28) can be solved as:

$$P_{E_2}^{RF,ASy}=\frac{\pi\sqrt{2}p}{4\xi\sqrt{\pi}}\exp\left(-\frac{\rho}{2\xi^2}\right)\sum_{k=0}^{\infty}\frac{(-1)^k q^{-(k+7/8)}}{k!\,(2\xi^2)^k\,\Gamma(1/8-k)\,\Gamma(1/2)} \tag{31}$$

Moreover, by invoking Eqs. (29) and (31) into Eq. (20), the asymptotic ABER for the concerned system can be expressed as:

$$\begin{aligned} ABER_{Asy} \;=\; & \frac{p}{2\sqrt{\pi}}\sum_{j=1}^{2}A_j\,(B_j)^{C_j}\frac{\Gamma(C_j)\,\Gamma(C_j/2+1/2)}{q^{(C_j/2)}\Gamma(1+C_j)} \\ & +\frac{\pi\sqrt{2}p}{4\xi\sqrt{\pi}}\exp\left(-\frac{\rho}{2\xi^2}\right)\sum_{k=0}^{\infty}\frac{(-1)^k q^{-(k+7/8)}}{k!\,(2\xi^2)^k\,\Gamma(1/8-k)\,\Gamma(1/2)} \\ & -\frac{\sqrt{2}p^2}{4\xi}\exp\left(-\frac{\rho}{2\xi^2}\right)\sum_{j=1}^{2}\sum_{k=0}^{\infty}\frac{A_j\,(B_j)^{C_j}(-1)^k q^{-(k+7/8+C_j/2)}\Gamma(C_j)\,\Gamma(C_j/2+1/2)}{k!\,(2\xi^2)^k\,\Gamma(1/8-k)\,\Gamma(1/2)\,\Gamma(1+C_j)} \end{aligned} \tag{32}$$

4. NUMERICAL RESULTS AND DISCUSSIONS

In this section, the numerical results of the system outage probability, ABER, and asymptotic expression under the heterodyne and IMDD detection techniques are presented. The UWOC is subjected to the following channel conditions detailed in [16] for air bubbles levels (BL(L/ min)) and temperature gradients (T(°C.cm)) as follows: For $BL = 2.4$ L/min and $T = 0.15$°C.cm ($\omega = 0.2877$, $\lambda = 0.4077$, $\alpha = 79.2682$, $\beta = 0.0156$) and for $BL = 16.5$ L/min and $T = 0.22$°C.cm ($\omega = 0.6527$, $\lambda = 0.1194$, $\alpha = 3.1458$, $\beta = 0.8439$). Except otherwise stated, the average SNR of the concerned system is set to be equal that is $\bar{\gamma} = \bar{\gamma}_{SR} = \bar{\gamma}_{RD}$.

The outage probability performance of the concerned system under the influence of optical turbulence is depicted in Figure 2 for the two detection schemes. The results show that the system performance deteriorates as the water air bubbles and temperature gradient increase due to stronger optical turbulence as a result of higher scintillation index. Also, the asymptotic results perfectly agreed with the analytical result at high SNR regime. This proved the tightness of the derived asymptotic expression. It is clearly observed that the heterodyne detection outperforms the IMDD detection under the same conditions. The results also show that the simulation results are well matched with the analytical results which confirm the correctness of the derived closed form outage probability expression.

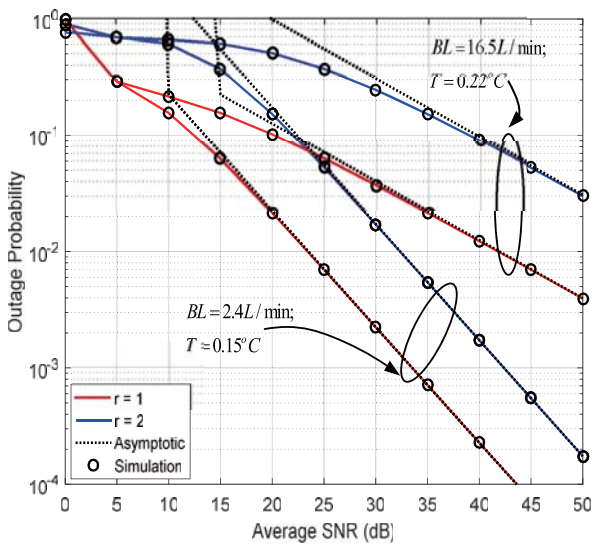

Figure 2. Impact of optical turbulence on the system outage performance under the two detection techniques when $N = 10$ and $\gamma_{th} = 5$ dB.

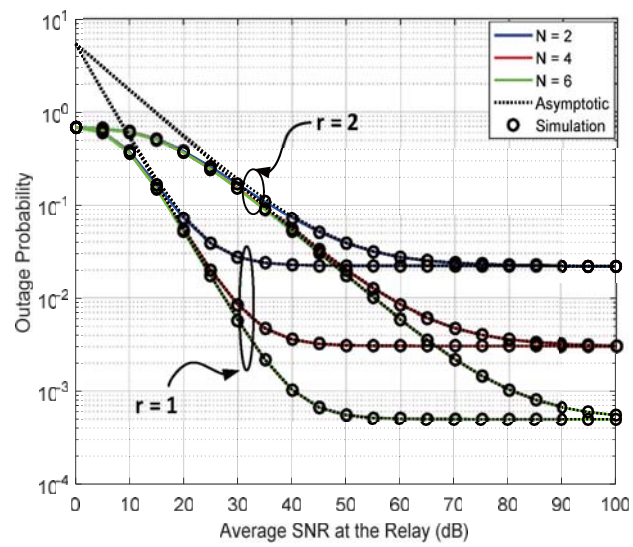

Figure 3. Outage performance as a function of $\bar{\gamma}_{RD}$ for different number of reflecting elements in RIS under the $BL = 16.5$ L/min and $T = 0.22$°C.cm when $\bar{\gamma}_{RD} = 10$ and $\gamma_{th} = 5$ dB.

In Figure 3, the impact of number of reflecting RIS elements as function of $\bar{\gamma}_{RD}$ is presented. It can be observed that the system outage improves as the number of reflecting RIS elements, N, increases. Also, the asymptotic results perfectly agreed with the analytical result at high SNR regime. It is clearly observed that the analytical results are perfectly matched with the simulated ones which justifies the accuracy of our derivation. At a particular number of RIS elements, the results demonstrate that heterodyne detection offers the system better performance than IMDD detection.

The effect of threshold SNR on the system outage performance is illustrated in Figure 4. The results show that the increase in threshold SNR worsens the system performance with heterodyne detection outperforming the IMDD detection. Moreover, the results show that both the simulated and asymptotic results perfectly agreed with the analytical results.

The system error performance as a function of $\bar{\gamma}_{RD}$ under different numbers of reflecting RIS elements for BPSK is demonstrated in Figure 5. The results depict that the system error performance is enhanced as the number of reflecting RIS elements increases. It can be deduced from the results

that the asymptotic results are well matched the analytical ones at high SNR regime which confirms the tightness of the derived close-form expression of the system ABER. The results also depict that simulation results are perfectly matched with the analytical results which justifies the accuracy of our derived ABER. It can be clearly observed that the heterodyne detection offers better performance than the IMDD detection.

The system error rate performance under different modulation schemes and optical turbulence is presented in Figure 6. The results show that as the water air bubbles and temperature gradient increase, the received intensity signal undergoes severe fluctuation which leads to increase in the system average error rate. In addition, the results depict that the BPSK modulation scheme outperforms the BFSK modulation scheme. It can be observed that the heterodyne detection offers the system better performance than IMDD detection.

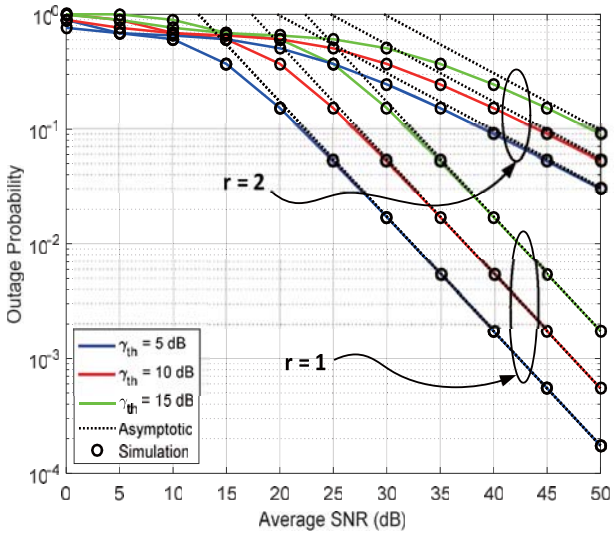

Figure 4. Effect of threshold SNR γ_{th} under $BL = 16.5\,\mathrm{L/min}$ and $T = 0.22°\mathrm{C.cm}$ when $N = 10$.

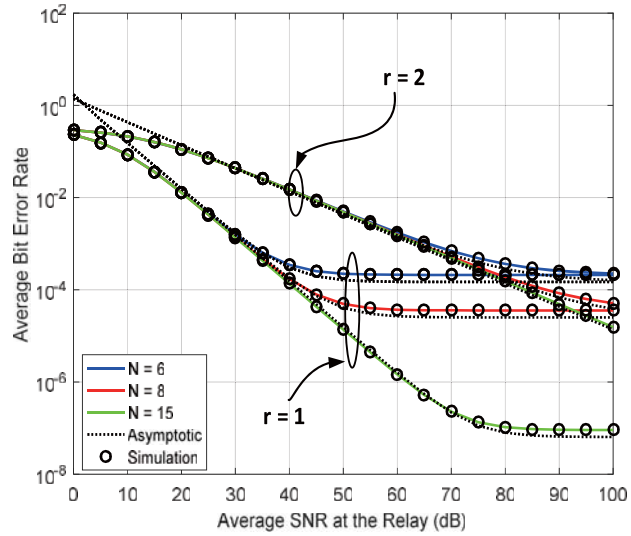

Figure 5. Error rate performance as a function of $\bar{\gamma}_{RD}$ under different number of reflecting RIS elements for BPSK when $\bar{\gamma}_{RD} = 5\,\mathrm{dB}$ at $BL = 16.5\,\mathrm{L/min}$ and $T = 0.22°\mathrm{C.cm}$.

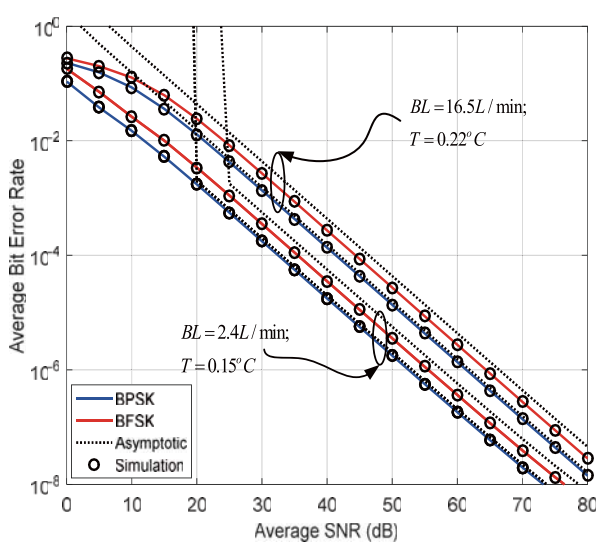

Figure 6. Error rate performance for different modulation schemes under different optical turbulence when $N = 10$.

5. CONCLUSION

The performance of a RIS-assisted UWOC system is investigated in this paper. The exact closed-form expressions of the concerned system outage probability and average bit error rate are derived. Also, in order to gain more performance insight, the asymptotic expression of the outage probability and the ABER are derived at high SNR. In addition, the system diversity gain is obtained through the derived asymptotic expression. It is demonstrated by the results that the analytical results perfectly agree with Monte-Carlo simulation results which justifies the accuracy of the derived exact expressions. Moreover, the results illustrate that the number of RIS elements and the optical turbulence caused by air bubbles and temperature significantly affect the system performance. It is also depicted that the heterodyne detection offers the system better performance than IMDD. In future research study, the effect of frequency dispersion on the performance of the concern system should be considered.

REFERENCES

1. Huang, C., A. Zappone, G. C. Alexandropoulos, M. Debbah, and C. Yuen, "Reconfigurable intelligent surfaces for energy efficiency in wireless communication," *IEEE Transactions on Wireless Communications Name*, Vol. 18, No. 8, 4157–4170, 2019.
2. Yang, L., Y. Yang, M. O. Hasna, and M.-S. Alouini, "Coverage, probability of SNR gain, and DOR analysis of RIS-aided communication systems," *IEEE Wireless Communications Letters*, 2020.
3. Basar, E., M. Di Renzo, J. De Rosny, M. Debbah, M.-S. Alouini, and R. Zhang, "Wireless communications through reconfigurable intelligent surfaces," *IEEE Access*, Vol. 7, 116753–116773, 2019.
4. Yang, L., W. Guo, and I. S. Ansari, "Mixed Dual-Hop FSO-RF Communication Systems Through Reconfigurable Intelligent Surface," *IEEE Communications Letters*, 2020.
5. Basar, E., "Transmission through large intelligent surfaces: A new frontier in wireless communications," *2019 European Conference on Networks and Communications (EuCNC)*, 112–117, IEEE, 2019.
6. Odeyemi, K. O., P. A. Owolawi, and O. O. Olakanmi, "Reconfigurable intelligent surface assisted mobile network with randomly moving user over Fisher-Snedecor fading channel," *Physical Communication*, 101186, 2020.
7. Nemati, M., J. Park, and J. Choi, "RIS-assisted coverage enhancement in millimeter-wave cellular networks," arXiv preprint arXiv:.08196, 2020.
8. Subrt, L. and P. Pechac, "Controlling propagation environments using intelligent walls," *2012 6th European Conference on Antennas and Propagation (EUCAP)*, 1–5, IEEE, 2012.
9. Tan, X., Z. Sun, D. Koutsonikolas, and J. M. Jornet, "Enabling indoor mobile millimeter-wave networks based on smart reflect-arrays," *IEEE INFOCOM 2018-IEEE Conference on Computer Communications*, 270–278, IEEE, 2018.
10. Wu, Q. and R. Zhang, "Beamforming optimization for wireless network aided by intelligent reflecting surface with discrete phase shifts," *IEEE Transactions on Communications Name*, Vol. 68, No. 3, 1838–1851, 2019.
11. Hu, S., K. Chitti, F. Rusek, and O. Edfors, "User assignment with distributed large intelligent surface (LIS) systems," *2018 IEEE 29th Annual International Symposium on Personal, Indoor and Mobile Radio Communications (PIMRC)*, 1–6, IEEE, 2018.
12. Ramavath, P. N., S. A. Udupi, and P. Krishnan, "High-speed and reliable underwater wireless optical communication system using multiple-input multiple-output and channel coding techniques for IoUT applications," *Optics Communications Name*, Vol. 461, 125229, 2020.
13. Kaushal, H. and G. Kaddoum, "Underwater optical wireless communication," *IEEE access Name*, Vol. 4, 1518–1547, 2016.
14. Zedini, E., A. Kammoun, H. Soury, M. Hamdi, and M.-S. Alouini, "Performance analysis of dual-hop underwater wireless optical communication systems over mixture exponential-generalized gamma turbulence channels," *IEEE Transactions on Communications*, 2020.

15. Saxena, P. and M. R. Bhatnagar, "A simplified form of beam spread function in underwater wireless optical communication and its applications," *IEEE Access Name*, Vol. 7, 105298–105313, 2019.
16. Zedini, E., H. M. Oubei, A. Kammoun, M. Hamdi, B. S. Ooi, and M.-S. Alouini, "Unified statistical channel model for turbulence-induced fading in underwater wireless optical communication systems," *IEEE Transactions on Communications Name*, Vol. 67, No. 4, 2893–2907, 2019.
17. Odeyemi, K. O. and P. A. Owolawi, "Wireless energy harvesting based asymmetric RF/FSO system with transmit antenna selection and receive diversity over M-distribution channel and non-zero boresight pointing error," *Optics Communications Name*, Vol. 461, 125219, 2020.
18. Lei, H., Y. Zhang, K.-H. Park, I. S. Ansari, G. Pan, and M.-S. Alouini, "Performance analysis of dual-hop RF-UWOC systems," *IEEE Photonics Journal Name*, Vol. 12, No. 2, 1–15, 2020.
19. Amer, M. and Y. Al-Eryani, "Underwater optical communication system relayed by $\alpha-\mu $ fading channel: Outage, capacity and asymptotic analysis," arXiv preprint arXiv:.04243, 2019.
20. Lei, H., Y. Zhang, K.-H. Park, I. S. Ansari, G. Pan, and M.-S. Alouini, "On the performance of dual-hop RF-UWOC system," *2020 IEEE International Conference on Communications Workshops (ICC Workshops)*, 1–6, IEEE, 2020.
21. Proakis, J. G. and M. J. I. Salehi, New York, *Digital Communications*, McGraw-Hill, 1995.
22. Yang, L. and Y. Yuan, "Secrecy outage probability analysis for RIS-assisted NOMA systems," arXiv preprint arXiv:.15902, 2020.
23. Wolfram, I., Research, Wolfram|One, Available: https://functions.wolfram.com/BesselTypeFunctions/BesselI/introductions/Bessels/ShowAll.html, 2020.
24. Gradshteyn, I. S. and I. M. Ryzhik, *Table of Integrals, Series, and Products*, Academic Press, 2014.
25. Adamchik, V. and O. Marichev, "The algorithm for calculating integrals of hypergeometric type functions and its realization in REDUCE system," *Proceedings of the International Symposium on Symbolic and Algebraic Computation*, 212–224, 1990.
26. Zedini, E., I. S. Ansari, and M.-S. Alouini, "Performance analysis of mixed Nakagami-m and Gamma–Gamma dual-hop FSO transmission systems," *IEEE Photonics Journal Name*, Vol. 7, No. 1, 1–20, 2014.
27. Yang, L., M.-S. Alouini, and I. S. Ansari, "Asymptotic performance analysis of two-way relaying FSO networks with nonzero boresight pointing errors over double-generalized gamma fading channels," *IEEE Transactions on Vehicular Technology Name*, Vol. 67, No. 8, 7800–7805, 2018.